



Ultrasonic-assisted adsorption of methylene blue on sumac leaves

Jale Gülen^{a,*}, Bora Akın^b, Mahmure Özgür^c

^aChemical Engineering Department, Yıldız Technical University, 34210 Esenler – Istanbul, Turkey, email: gulenj@yildiz.edu.tr

^bChemical Engineering Department, Çankırı Karatekin University, 18200 Çankırı, Turkey, email: mboraakin@gmail.com

^cChemistry Department, Yıldız Technical University, 34210 Esenler – Istanbul, Turkey, email: mozgur@yildiz.edu.tr

Received 13 February 2014; Accepted 8 March 2015

ABSTRACT

Sumac leaves (SL) (*Rhus coriaria* L.) were investigated as a low-cost and effective bioadsorbent for the adsorption of methylene blue (MB) from aqueous solution. In this study, the effects of initial dye concentration, initial solution pH, and phases contact time were investigated. The equilibrium was attained in half an hour. The Langmuir, Freundlich, and Temkin adsorption models were evaluated using the experimental data and the experimental results showed that the Langmuir and Temkin models fit better than the Freundlich model. The maximum dye adsorption capacity was found as 5.8 mg/g from the Langmuir isotherm model. The value of the monolayer saturation capacity of SL was comparable to the adsorption capacities of some other adsorbent materials for MB. The adsorption rate data were analyzed according to the pseudo-first-order kinetic model, pseudo-second-order kinetic model, and intraparticle diffusion model. It was found that the adsorption reaction progressed as a pseudo-second-order kinetic model and intraparticle diffusion was also effective in the process.

Keywords: Adsorption; Biosorbent; Isotherms; Kinetics; Methylene blue; Sumac leaves; Langmuir; Freundlich; Temkin; Ultrasonic-assisted

1. Introduction

Nowadays, the amount of environmental problems increases day by day. The destruction of forests, erosion, increasing population, decreasing green areas, distorting seashores, increasing chemical applications, and shortage of energy sources cause these environmental problems both in Turkey and the world. Industrialization and urbanization caused the air, water, and soil pollutions, which are above the biological tolerance limits [1].

Industrial effluents, especially dyeing industries, cause environmental pollution [2]. Dyes are resistant

to light, many chemicals, oxidizing agents, and heat due to their strong chemical structure. They are biologically non-degradable and therefore difficult to decolorize once they are released into the aquatic environment [3]. Disposal of this polluted water into receiving bodies can be toxic to aquatic life. They are mutagenic and carcinogenic substances, and cause severe damage to the kidneys, reproductive system, liver, brain, and nervous system of human beings [2]. From the point of economic considerations, application of coagulation, reverse osmosis, flotation, precipitation, etc. is very difficult to wastewater containing dyes discharged from the textile industry. Adsorption has gained prominent importance due to efficiency in the

*Corresponding author.

removal of pollutants from effluents instead of the above conventional purification methods [4,5].

Activated carbons have been popular adsorbents in wastewater treatment processes [6–8]. But it is quite expensive and also has problems associated with regeneration. On the other hand, there is a growing interest in using low-cost materials for the adsorption of dyes. A wide variety of materials such as peat [9], palm-fruit [10], silica fumes [11], natural zeolite [12], montmorillonite and kaolinite [13], clay [14,15], activated clay [16], and fuller earth [17] are employed as low-cost adsorbents instead of activated carbons.

Recently, the interest on biomaterials and especially tannins has been growing and some attractive results have been obtained in the adsorption of some metals by tannin adsorbents [18]. Tannins are widely distributed in nature and have multiple adjacent polyhydroxyphenyl groups in their chemical structure, which have extremely high affinity for heavy metal ions [19], all proteins, and other macromolecules like polysaccharides. Sumac Leaves (*Rhus coriaria* L.) (SL) is a shrub, which reaches 3–4 m in height in the wild. The main compounds present in *Rhus* family are hydrolysable gallotannins. Turkish sumac tannin (hydrolysable tannins) is illustrated in Fig. 1 whose basic structure is of flavan-3-ols [20]. In this study, SL were considered for the treatment of aqueous polluted solution because of two significant reasons. Firstly, sumac tree is widely grown in the high lands of our country and thus the adsorbent can be prepared and used wherever the problem exists. Secondly, SL contain hydrolysable gallotannins which are highly beneficial due to their properties like antibacterial, antimicrobial, antibite, and anticoloring in nature [21]. MB is selected as a model compound for evaluating the potential of SL to remove dye from wastewaters. MB is a cationic dye, which is most commonly used for coloring paper, temporary hair colorant, dyeing cottons, wools, and so on. This dye is not strongly hazardous, but it can cause some harmful effects.

Environmental sonochemistry has also been growing in recent years [22–24]. The developed cavitation reduces microvortex motion of reactant solution on the surface of particles and also increases a stirring up

role in the reactant system. Presence of ultrasound increases mass transfer rate by reducing diffusion resistance [25–27].

The focus of the present research is to characterize adsorption properties of methylene blue (MB) via sonication on the SL as a low-cost and ecofriendly adsorbent. The adsorption isotherms, kinetics, and pH effects have also been searched from the point of adsorption yield.

2. Materials and methods

2.1. Materials

A monovalent cationic dye, MB was selected for adsorption studies. It was purchased from Sigma-Aldrich. The chemical formula of MB ($C_{16}H_{18}N_3SCl$) is given in Fig. 1.

SL were supplied from Manisa city (Aegean region of Turkey). Turkish sumac tannin (hydrolysable tannins) is illustrated in Fig. 2 [29].

The leaves were dried at room temperature. They were grounded and sieved, and the fraction of particles $<300\ \mu\text{m}$ was used for adsorption studies. Samples were stored in an air-tight plastic containers. The surface area of the SL, measured using Branauer–Emmet–Teller (BET) adsorption technique using a Micromeritics Gemini VII 2390 V1.03 (Micromeritics Co., USA), was $1.0312 \pm 0.0926\ \text{m}^2/\text{g}$ (Fig. 3).

2.2. Apparatus

The Bandelin model RK 100H operating at a fixed frequency of 20 kHz and 250 W ultrasonic bath was used in the adsorption experiments. The pH values were recorded on Hach sension pH meter pH 3 (Criso, Spain). The absorbance data were performed using ATI/UNICAM UV/V spectrophotometer at $\lambda_{\text{max}} = 665\ \text{nm}$. The FTIR spectra (A Mattson 1000 Spectrometry) were used to characterize the functional groups of the SL and MB adsorbed SL.

2.3. Adsorption studies

2.3.1. Calibration step

The MB stock solution was prepared by dissolving 0.01 g MB in 100 ml demineralized water. This stock solution was diluted to different concentrations for obtaining absorbance calibration data. For this purpose, the samples (0.2, 0.4, 0.6, ..., 3.6, 3.8 mL) were diluted to 50 mL with deionized water. At the calibration step before UV analyzing, 1 mL solution was diluted to 10 mL again for better absorption values.

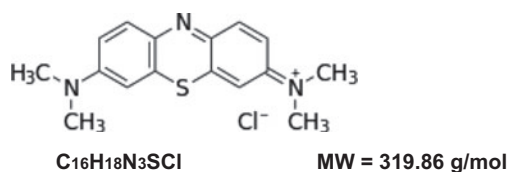


Fig. 1. The chemical structure of MB [28].

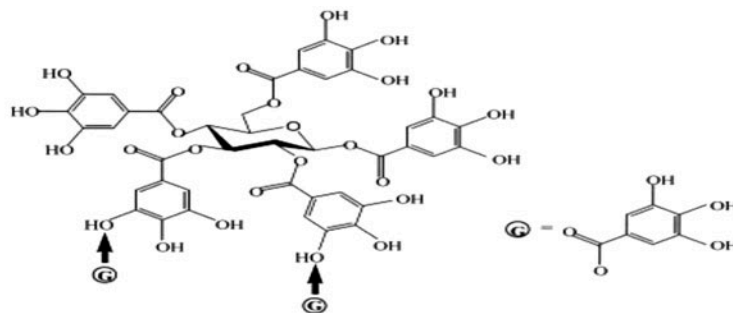


Fig. 2. Sumac (*R. coriaria* L.) and chemical structure of Turkish Sumac tannin [29].

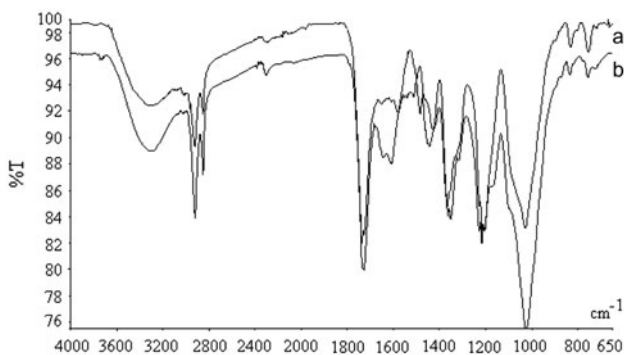


Fig. 3. FTIR spectra (a) SL and (b) MB adsorbed SL.

The calibration curve was drawn by plotting these values at the selected wavelength ($\lambda = 665$ nm) against the corresponding concentration of MB solution. Each measurement was repeated three times. The concentration values were calculated from equation ($y = 0.3741X + 0.0631$, $R^2 = 0.99$).

2.3.2. Experimental step

For the adsorption experiments, 1, 1.5, 2, 2.5, 3, and 3.5 mL of stock solutions were diluted to 50 mL with distilled water. The corresponding concentrations of the solutions were 2, 3, 4, 5, 6, and 7 $\mu\text{g mL}^{-1}$. The variation of adsorbent dose was kept constant and chosen as 0.1 g during the experimental study. The adsorption experiments were carried out in 100 mL stoppered polyethylene conical flasks filled with 50 mL diluted MB solution. The reaction mixture was stirred for different time intervals with sonication of an ultrasonic Bandelin brand bath until adsorption equilibrium was attained. The adsorption data were measured in five minutes intervals. Five milliliters supernatant was diluted to 10 mL, and the liquid phase was centrifuged at 1,000 rpm for 3 min. The

experiments were performed at 25°C with different pH values to see the effect of pH changes on the adsorption process.

3. Results and discussion

3.1. Adsorbent characterization

The FTIR spectra of SL (a) and MB adsorbed SL (b) are shown in Fig. 3. The broad peak in the region of 3,400–3,200 cm^{-1} is characteristic of the –OH stretchings of the phenolic and methylol group of tannin. The peaks at approximately 1,300 and 1,000 cm^{-1} in the spectrum of tannin belong to phenol groups [30]. The absorption bands between 1,689 and 1,459 cm^{-1} are characteristic of the elongation of the aromatic –C=C– bonds. The deformation vibration of the carbon–carbon bonds in the phenolic groups absorbs in the region of 1,520–1,400 cm^{-1} . Also, the FTIR spectra of SL (a) and MB adsorbed SL (b) are similar and this is the indicator that the adsorption progressed as a physical type.

3.2. Contact time and initial adsorbate concentration

The effect of initial concentration of MB on the MB adsorption by SL is shown in Figs. 4 and 5. It can be seen that the amount of MB adsorbed (mg/g) increased with increased MB concentration and remained constant after equilibrium time. The concentration supplies an important driving force to overcome all mass transfer resistance of the MB between the aqueous and solid phases. Hence, a higher initial concentration of MB will increase the adsorption process. The equilibrium sorption capacity of the SL increased with an increase in initial MB concentration, while the removal % of MB showed the opposite trend. When the initial MB concentration increased from 2 to 7 $\mu\text{g/mL}$, the loading capacity increased from 0.85 to 3.20 mg/g and the percentage removal

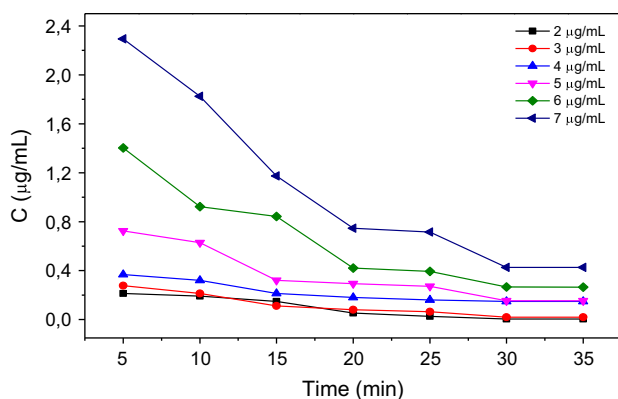


Fig. 4. Concentration variations of several MB solutions with contact time at 25°C.

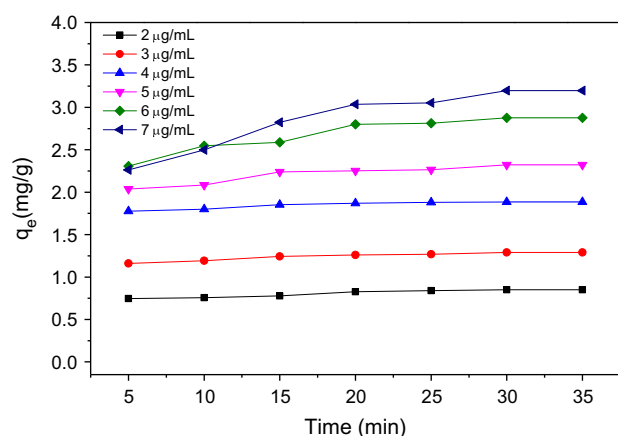


Fig. 5. Effect of phases contact time on MB adsorption by SL, experimental conditions: pH 5; adsorbent dose 0.1 g/50 mL; T 25°C.

decreased from 99.70 to 93.75%. This is the similar behavior that was seen for the adsorption of MB onto agricultural waste adsorbent [31], onto *Parthenium hysterophorus* [32] and onto bamboo-based activated carbon [33]. The equilibrium was attained in half an hour.

3.3. Effect of solution pH on MB adsorption

The effect of solution pH on the equilibrium removal capacity of SL was studied at 4 µg/mL initial MB concentration and 25°C temperature between pH values of 2 and 12. As shown in Fig. 6, the MB removal was found to increase with an increase in pH. It increased from 1.62 to 1.73 µg/g for an increase in pH from 2 to 8. But further increase in pH from 8 to 10 will not affect the adsorption. The result

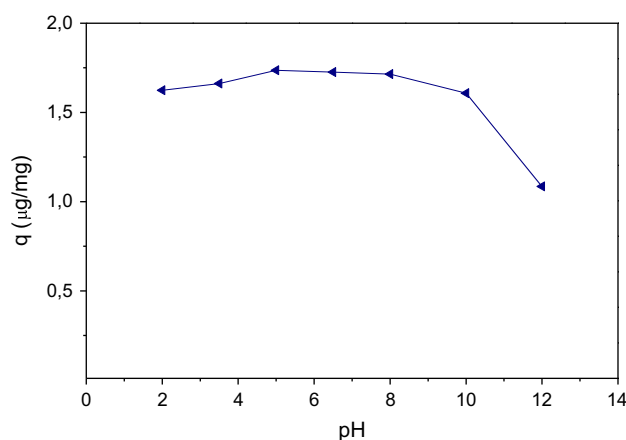


Fig. 6. Effect of initial solution pH on the adsorption of MB by SL, experimental conditions: adsorbent dose 0.1 g/50 mL; T 25°C; contact time 0.5 h; Co 4 µg/mL.

indicated that acidic pH supported the biosorption of dye on SL. A similar trend was reported for the adsorption of MB onto a novel agricultural waste [31], *Posidonia oceanica* fibers [34] and wheat shells [35].

pH_{pzc} is found as 2. The effect of pH was explained in terms of charge zero. At lower pH like 2, the surface charge may be positively charged, thus making hydrogen ions to compete effectively with MB cations causing a decrease in the amount of MB adsorbed. At higher pH, the surface of SL may be negatively charged that enhance the positively charged MB cations through electrostatic force attraction. A similar trend was observed for the adsorption of MB onto *Posidonia oceanica* (L.) fibers [34], rice straw derived char [36], and yellow passion fruit peel [37].

At pH values lower than pH_{pzc} , the surface charge of the solid turns into positive and adsorption of cations is not favorable. The hydrogen ions compete with dye ions upon the active sites; that is why the adsorption becomes limited. Above the pH_{pzc} , the surface charge of the adsorbent is negative, and binding of cations is favorable.

The reaction mechanism between dye and tannin is represented below (Fig. 7).

3.4. Adsorption isotherms

In order to establish the most appropriate correlations for the equilibrium data from the point of designing the adsorption system, the Langmuir, Freundlich, and Temkin isotherm models were tested. The applicability of the isotherm equations was tested by comparing the correlation coefficients, R^2 .

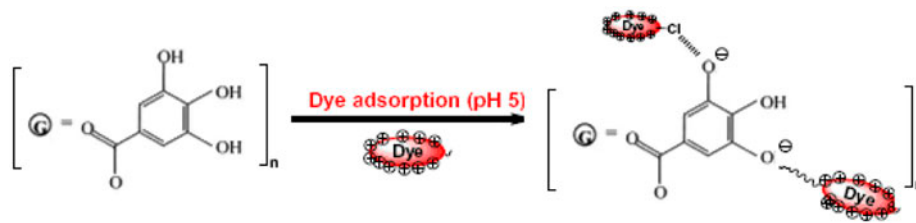


Fig. 7. The reaction mechanism between MB and tannin [38,39].

The Langmuir adsorption [40] model is based on the assumption that maximum adsorption corresponds to a saturated monolayer of the solute molecules on the adsorbent surface. The linear form of the Langmuir equation is described by

$$\frac{C_e}{q_e} = \left(\frac{1}{Q_0 b}\right) + \left(\frac{1}{Q_0}\right)C_e \tag{1}$$

where C_e (mg/L) is the equilibrium concentration of the adsorbate, q_e (mg/g) is the amount of adsorbate per unit mass of adsorbent, Q_0 and b are Langmuir constants related to adsorption capacity (mg/g) and rate of adsorption (L/mg), respectively. The linear plot of specific adsorption (C_e/q_e) against the equilibrium concentration (C_e) (Fig. 8) shows that the adsorption obeys the Langmuir model. The Langmuir constants Q_0 and b were determined from the slope and intercept of the plot and are represented in Table 1. The R^2 values (0.99) suggest that the Langmuir isotherm provides a good fit to the isotherm data. A similar observation was reported for adsorption of MB onto fly ash [41], a natural silkworm pupa [42], both cedars saw dust and crushed brick [43] and rice husk [44].

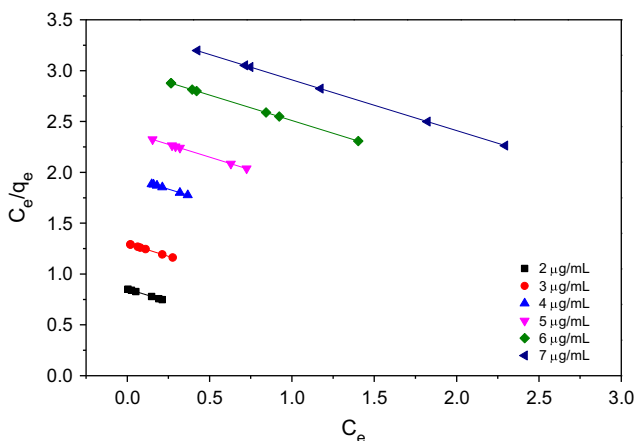


Fig. 8. Linearized Langmuir isotherm for MB adsorption onto SL.

Table 1

The constants of isotherm models of 4 µg/mL MB solutions

Langmuir isotherm	
Q_0 (mg/g)	0.58
B (L/mg)	0.009
R^2	0.99
Freundlich isotherm	
K_F (mg/g(L/mg) ^{1/n})	5.3
n	17.86
R^2	0.72
Temkin isotherm	
b_T (J/mol)	271.66
K_T (L/g)	1.20
R^2	0.99

The essential characteristics of the Langmuir isotherm can be expressed in terms of a dimensionless constant separation factor R_L [45] given by equation.

$$R_L = \frac{1}{1 + bC_0} \tag{2}$$

where C_0 (mg/L) is the highest initial concentration of adsorbent, and b (L/mg) is the Langmuir constant. The parameter R_L indicates the nature of shape of the isotherm accordingly:

$R_L > 1$	Unfavorable adsorption
$0 < R_L < 1$	Favorable adsorption
$R_L = 0$	Irreversible adsorption
$R_L = 1$	Linear adsorption

The value of R_L in this study has been found to be 0.9653 at 25°C showing that the adsorption of MB on SL is favorable at the studied temperature. The Freundlich isotherm [46] is the earliest known relationship describing the sorption equation. The fairly satisfactory empirical isotherm can be used for non-ideal sorption

that involves heterogeneous surface energy systems and is expressed by the following Eq. (3)

$$q_e = K_F C_e^{1/n} \tag{3}$$

where K_F (mg/g(L/mg)^{1/n}) is roughly an indicator of the adsorption capacity and $1/n$ is the adsorption intensity. In general, as the K_F value increases the adsorption capacity of adsorbent increases. The magnitude of the exponent, $1/n$ gives an indication of the favorability of adsorption. Value of $n > 1$ represents favorable adsorption condition [47,48]. The linear form of Eq. (3) is

$$\log q_e = \log K_F + \left(\frac{1}{n}\right) \log C_e \tag{4}$$

values of K_F and n are calculated from the intercept and slope of the plot (Fig. 9) are listed in Table 1. The R^2 value (0.72) is lower than Langmuir isotherm. A high R^2 (0.997) value was found for the adsorption of MB onto natural illitic clay [47]. The value of Freundlich exponent n (17.86) is in the range of $n > 1$, indicating a favorable adsorption [48,49].

Temkin isotherm is valid for that the enthalpy of adsorption changes linearly with coverage due to adsorbent–adsorbate interactions [50]. The adsorption is a uniform distribution of binding energies, up to some maximum binding energy. The Temkin isotherm equation in linear form is given as

$$q_e = \frac{RT}{bT} \ln KT + \frac{RT}{bT} \ln C_e \tag{5}$$

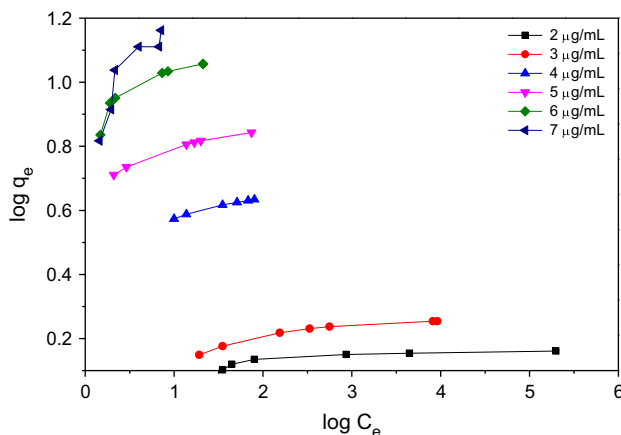


Fig. 9. Linearized Freundlich isotherm for MB adsorption onto SL.

where R is universal gas constant (8.314 J/(mol K)), T (K), absolute temperature, K_T (L/g), equilibrium binding constant, b_T (J/mol), related to heat of adsorption. The values b_T and K_T were determined from the slope and intercept of Fig. 10 and given in Table 1. The R^2 value is rather high (0.99) for MB removal by SL. The similar high R^2 values were seen for adsorption of MB by bentonite [51] and palm leaves [52].

The best equilibrium model was determined based on the linear square regression correlation coefficient R^2 . From Table 1, it was observed that the equilibrium sorption data were best represented by the Langmuir and Temkin isotherms. The best fit isotherm expressions confirm the monolayer coverage process of MB onto SL. A similar result was reported for adsorption of MB onto sewage sludge [53] and a novel agricultural waste adsorbent [31].

Table 2 lists a comparison of maximum monolayer adsorption capacity of MB on various adsorbents. Sumac leaf is found to have an adsorption capacity of 5.8 mg/g and this indicates that it could be considered as a promising material for the removal of MB from aqueous solution. These SL were also used by Dulger et al. in the removal of basic dye from aqueous solution. The maximum adsorption capacity was reached to 151.69 mg/g for 600 mg/L initial MB concentration [54]. The equilibrium time was found as 120 min. But in this study, it was found as 30 min. This shows the distinctive feature of ultrasound effect. The experimental conditions play an important role for calculating the adsorption capacity [31,55].

3.5. Adsorption kinetics

Pseudo-first-order and pseudo-second-order models were applied to test experimental data and thus elucidated the kinetic adsorption process. Lagergren proposed an equation for adsorption analysis that is the pseudo-first-order kinetic model [57] (Fig. 10).

$$\log(q_e - q_t) = \log q_e - \frac{k_1}{2.303} t \tag{6}$$

Table 2
The adsorption capacity of various adsorbents

Adsorbent	Q_{max} (mg/g)	Ref.
Sumac leaves	5.8	Present study
Raw <i>Posidonia oceanica</i> fibers	5.56	[34]
Yellow passion fruit peel	0.0068	[37]
Egg shell	0.80	[56]
Egg shell membrane	0.24	[56]

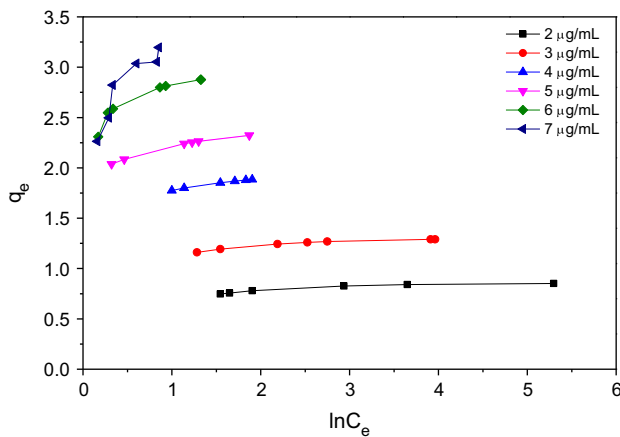


Fig. 10. Linearized Temkin isotherm for MB adsorption onto SL.

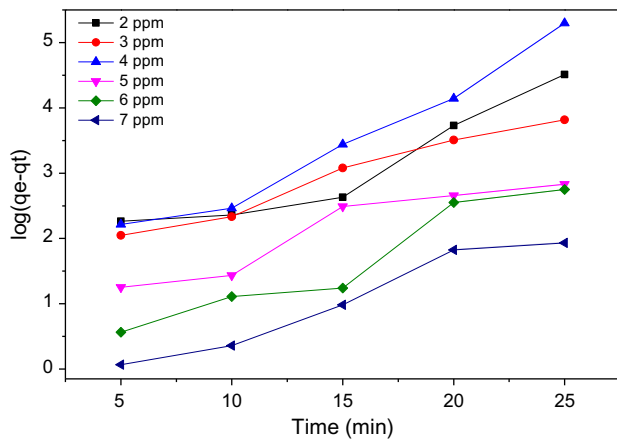


Fig. 11. Linearized pseudo-first-order kinetic plots for MB adsorption on SL of various concentrations, experimental conditions: adsorbent dose 0.1 g/50 mL; pH 5.

where k_1 (1/min) is the rate constant, q_e (mg/g) is the amount of solute adsorbed on the surface at equilibrium, and q_t (mg/g) is the amount of solute adsorbed

at any time. The value of k_1 for MB adsorption by SL was determined from the plot of $\log(q_e - q_t)$ against t (Fig. 11). The parameters of pseudo-first-order model are summarized in Table 3.

Although, the correlation coefficients (R^2) are generally greater than 0.893 for all initial concentrations under the limit of the experimental q_e for the pseudo-first-order kinetic model. As such, the adsorption of MB on SL cannot be described best by the pseudo-first-order kinetic. In many cases, the first-order Lagergren equation does not fit well to the whole range of contact time and is applicable over the initial stage of the adsorption process generally [58]. So, the pseudo-second-order kinetic model [48,59] was used to study the adsorption kinetic of this system

$$\frac{t}{q_t} = \frac{1}{k_2 q_e^2} + \left(\frac{1}{q_e}\right)t \tag{7}$$

where k_2 (g/mgmin) is the second-order rate constant. The q_e and k_2 are calculated from the slope and intercept of the plots t/q_t vs. t (Fig. 12).

The constant k_2 is used to calculate the initial sorption rate h (mg/gmin), as $t > 0$ as follows:

$$h = k_2 q_e^2 \tag{8}$$

The pseudo-second-order rate constants k_2 , the calculated h values, and the corresponding linear regression correlation coefficients R^2 are given in Table 3. The R^2 values were found to be in the range of (0.951–1.000). Besides, the variations between the calculated q_e and experimental q_e were very minimal for this model.

The high correlation coefficients and high agreement that exist between the calculated and experimental q_e values of the pseudo-second-order kinetic model over the other model renders it best in the adsorption of MB on SL. This confirms that the sorption data are

Table 3

Comparison of the pseudo-first-order, pseudo-second-order adsorption rate constant, and calculated and experimental q_e values obtained at different initial MB concentrations

Co (μg/mL)	Pseudo-first-order kinetic model				Pseudo-second-order kinetic model			
	$q_{e,exp}$ (mg/g)	$q_{e,cal}$ (mg/g)	k_1 (1/min)	R^2	$q_{e,cal}$ (mg/g)	k_2 (g/mgmin)	R^2	h (mg/gmin)
2	0.851	21.883	0.2701	0.893	0.876	0.8746	0.997	0.670
3	1.290	34.930	0.2169	0.977	1.416	0.5699	0.951	1.143
4	1.885	14.454	0.3611	0.966	1.915	1.0408	1.000	3.818
5	2.323	6.593	0.2017	0.891	2.597	0.1860	0.989	1.254
6	2.877	1.251	0.2667	0.926	3.001	0.1898	0.998	1.710
7	3.197	3.350	0.2393	0.955	3.436	0.0945	0.996	1.116

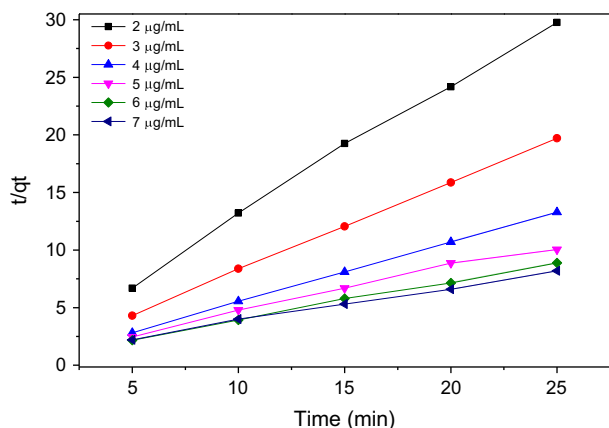


Fig. 12. Linearized pseudo-second-order kinetic plots for MB adsorption on SL of various concentrations, experimental conditions: adsorbent dose 0.1 g/50 mL; pH 5.

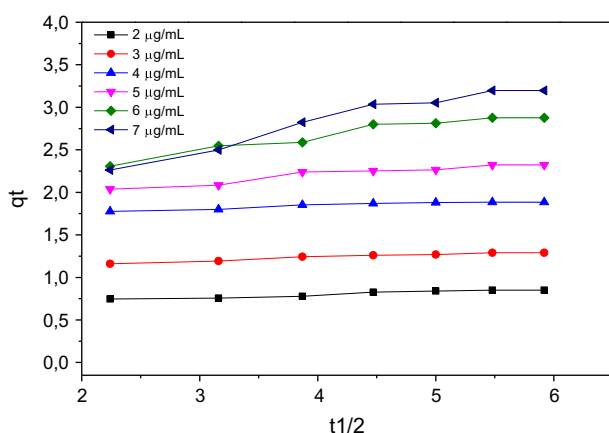


Fig. 13. Linearized intraparticle diffusion kinetic plots for MB adsorption on SL, experimental conditions: adsorbent dose 0.1 g/50 mL; pH 5.

represented well by the pseudo-second-order kinetic for the entire sorption period. The increase in values of the initial adsorption rates, h (Table 3) with an increase in the initial MB concentration could be attributed to the increase in the driving force for mass transfer, allowing more MB molecules to reach the surface of the adsorbents in a shorter period of time [60,61].

The kinetic results were further analyzed by the intraparticle diffusion model to elucidate the diffusion phenomenon [62].

$$q_t = k_{id}t^{1/2} + C \quad (9)$$

where C is the intercept and k_{id} is the intraparticle diffusion rate constant ($\text{mg/gmin}^{0.5}$), which is evaluated from the slope of the linear plot of q_t versus $t^{1/2}$

(Fig. 13). If the regression of q_t versus $t^{1/2}$ is linear and passes through the origin, intraparticle diffusion is the sole rate-limiting step [63]. The first sharper region is the instantaneous adsorption or external surface adsorption for intraparticle diffusion plots. The second region is the gradual adsorption stage, where intraparticle diffusion is the rate limiting. In some cases, there is a third region that is the final equilibrium stage, where intraparticle diffusion starts to slow down due to the extremely low adsorbate concentrations left in the solutions [64]. As seen from Fig. 13, the plots were not linear over the experimental time range, implying that more than one process affected the adsorption phenomenon.

4. Conclusions

The results showed the potential of SL to be a low-cost adsorbent for removal MB from aqueous solutions. The optimum biosorption conditions were found as the following: contact time: half an hour; initial pH: 5; initial dye concentration: 4 µg/mL; biosorbent dose: 0.1 g/50 mL; and temperature: 25°C. Equilibrium data were in good consistency with Langmuir and Temkin isotherm models. The monolayer adsorption capacity was 5.8 mg/g at 25°C for 4 µg/mL MB solution. The value of the separation factor, R_L , indicated the MB/SL system was a favorable adsorption. The rate orders of pseudo-first-order kinetic and pseudo-second-order kinetic models for the sorption of MB onto SL were discussed, too. The kinetic modeling study was the indicator that the experimental data followed the pseudo-second-order model, suggesting a chemisorption reaction. The FTIR spectra of the SL and MB absorbed SL were the indicator of physical type adsorption process.

Acknowledgments

This study is supported by the Research Fund of Yıldız Technical University YTU BAPK Project, 2011-07-01-GEP02.

References

- [1] K. Turhan, C. Ekinçi Doğan, G. Akçin, A. Aslan, Biosorption of Au(III) and Cu(II) from aqueous solution by a non living usnea longissima biomass, *Fresenius Environ. Bull.* 14(12) (2005) 1129–1135.
- [2] K. Kadirvelu, M. Kavipriya, C. Karthika, M. Radhika, N. Vennilamani, S. Pattabhi, Utilization of various agricultural wastes for activated carbon preparation and application for the removal of dyes and metal ions from aqueous solutions, *Bioresour. Technol.* 87(1) (2003) 129–132.

- [3] T. Robinson, B. Chandran, P. Nigam, Effect of pretreatments of three waste residues, wheat straw, corncobs and barley husks on dye adsorption, *Bioresour. Technol.* 85(2) (2002) 119–124.
- [4] Q. Sun, L. Yang, The adsorption of basic dyes from aqueous solution on modified peat resin particle, *Water Res.* 37(7) (2003) 1535–1544.
- [5] A.S. Özcan, A. Özcan, Adsorption of acid dyes from aqueous solutions onto acid activated bentonite, *J. Colloid Interface Sci.* 276 (2004) 39–46.
- [6] R.A. Davies, H.J. Kaempf, M.M. Clemens, Granular carbon for the treatment of textile effluents, *Chem. Ind.* 9 (1973) 827–831.
- [7] P.R.B. Kulkarni, A.S. Bal, A.G. Bhole, A.V. Bhoi, Color removal by granular activated carbon, *J. AWWA* 18 (1986) 244–273.
- [8] G.M. Walker, L.R. Weatherley, Adsorption of acid dyes on to granular activated carbon in fixed beds, *Water Res.* 31 (1997) 2093–2101.
- [9] G. Mc Kay, S.J. Allen, Single resistance mass transfer models for adsorption of dyes on peat, *J. Sep. Process. Technol.* 4 (1980) 1–7.
- [10] M.M. Nassar, M.F. Hamoda, G.H. Radwan, Adsorption equilibria of basic dyestuff onto palm-fruit bunch particles, *Water Sci. Technol.* 32 (1995) 27–32.
- [11] S.V. Mohan, V.V.S. Mamatha, J. Karthikeyan, Removal of color from acid and direct dyes by adsorption on to silica fumes, *Fresenius Environ. Bull.* 7 (1998) 51–58.
- [12] V. Meshko, L. Markovska, M. Mincheva, A.E. Rodrigues, Adsorption of basic dyes on granular activated carbon and natural zeolite, *Water Res.* 35 (2001) 3357–3366.
- [13] O. Yavuz, A.H. Aydın, The removal of acid dye from aqueous solution by different adsorbents, *Fresenius Environ. Bull.* 11 (2002) 377–383.
- [14] S.H. Lin, Ruey-Shin Juang, Y. Wang, Adsorption of acid dye from water onto pristine and acid-activated clays in fixed beds, *J. Hazard. Mater.* 113 (2004) 195–200.
- [15] J. Gülen, Z. Altın, M. Özgür, Adsorption of amitraz on the clay, *Am. J. Eng. Res.* 2(6) (2013) 1–8.
- [16] J. Gülen, F. Turak, M. Ozgur, Removal of amitrole by activated clay, *Int. J. Mod. Chem.* 2(2) (2012) 47–56.
- [17] G. Atun, G. Hisarli, W.S. Sheldrick, M. Muhler, Adsorptive removal of methylene blue from colored effluents on fuller's earth, *J. Colloid Interface Sci.* 261 (2003) 32–39.
- [18] M.R. Sohrabi, M. Ghavam, Photocatalytic degradation of Direct Red 23 dye using UV/TiO₂: Effect of operational parameters, *J. Hazard. Mater.* 153 (2008) 1235–1239.
- [19] M. Sleiman, D.L. Vildoza, C. Ferronato, J.M. Chovelon, Photocatalytic degradation of azo dye Metanil Yellow: Optimization and kinetic modeling using a chemometric approach, *Appl. Catal. B: Environ.* 77 (2007) 1–11.
- [20] M. Abbasi, N.R. Asl, Sonochemical degradation of Basic Blue 41 dye assisted by nanoTiO₂ and H₂O₂, *J. Hazard. Mater.* 153 (2008) 942–947.
- [21] N. Zaghbani, A. Hafiane, M. Dhahbi, Removal of Safranin T from wastewater using micellar enhanced ultrafiltration, *Desalination* 222 (2008) 348–356.
- [22] M.H. Entezari, A. Heshmati, A. Sarafraz-yazdi, A combination of ultrasound and inorganic catalyst: removal of 2-chlorophenol from aqueous solution, *Ultrason. Sonochem.* 12 (2005) 137–141.
- [23] S. Vajnhandl, A.M. Le Marechal, Case study of the sonochemical decolouration of textile azo dye Reactive Black 5, *J. Hazard. Mater.* 141 (2007) 329–335.
- [24] A.B. Pandit, M. Sivakumar, Ultrasound enhanced degradation of Rhodamine B: Optimization with power density, *Ultrason. Sonochem.* 8 (2001) 233–240.
- [25] W. Zheng, M. Maurin, M.A. Tarr, Enhancement of sonochemical degradation of phenol using hydrogen atom scavengers, *Ultrason. Sonochem.* 12 (2005) 313–317.
- [26] B.S. Schueller, R.Y. Yang, Ultrasound enhanced adsorption and desorption of phenol on activated carbon and polymeric resin, *Ind. Eng. Chem. Res.* 40 (2001) 4912–4918.
- [27] S. Sonawane, P. Chaudhari, S. Ghodke, S. Phadtare, S. Meshram, Ultrasound assisted adsorption of basic dye onto organically modified bentonite (nanoclay), *J. Sci. Ind. Res.* 68 (2009) 162–167.
- [28] Available from: http://en.wikipedia.org/wiki/methylene_blue (accessed December 2014).
- [29] A. Zalacain, M. Prodanov, M. Carmona, G.L. Alonso, Optimisation of extraction and identification of gallotannins from sumac leaves, *Biosyst. Eng.* 84 (2003) 211–216.
- [30] J.M. Garro-Galvez, M. Fechtal, B. Riedl, Gallic acid as a model of tannins in condensation with formaldehyde, *Thermochim. Acta* 274 (1996) 149–163.
- [31] B.H. Hameed, R.R. Krishni, S.A. Sata, A novel agricultural waste adsorbent for the removal of cationic dye from aqueous solutions, *J. Hazard. Mater.* 162 (2009) 305–311.
- [32] H. Lata, V.K. Garg, R.K. Gupta, Removal of a basic dye from aqueous solution by adsorption using *Parthenium hysterophorus*: An agricultural waste, *Dyes Pigm.* 74 (2007) 653–658.
- [33] B.H. Hameed, A.T.M. Dm, A.L. Ahmad, Adsorption of methylene blue onto bamboo-based activated carbon: Kinetics and equilibrium studies, *J. Hazard. Mater.* 141 (2007) 819–825.
- [34] M.C. Ncibi, B. Mahjoub, M. Seffen, Kinetic and equilibrium studies of methylene blue biosorption by *Posidonia oceanica* (L.) fibres, *J. Hazard. Mater.* 139 (2007) 280–285.
- [35] Y. Bulut, H. Aydın, A kinetics and thermodynamics study of methylene blue adsorption on wheat shells, *Desalination* 194 (2006) 259–267.
- [36] B.H. Hameed, M.I. El-Khaiary, Kinetics and equilibrium studies of malachite green adsorption on rice straw derived char, *J. Hazard. Mater.* 153 (2008) 701–708.
- [37] F.A. Pavan, A.C. Mazzocato, Y. Gushikem, Removal of methylene blue dye from aqueous solutions by adsorption using yellow passion fruit peel as adsorbent, *Bioresour. Technol.* 99 (2008) 3162–3165.
- [38] M. Özacar, C. Soykan, A. Şengül, Studies on synthesis, characterization and metal adsorption on mimosa and valonia tannin resins, *J. Appl. Polym. Sci.* 102 (2006) 786–797.
- [39] G.Z. Kyzas, P.I. Siafaka, E.G. Pavlidou, K.J. Chrissafis, D.N. Bikiaris, Synthesis and adsorption application of succinyl-grafted chitosan for the simultaneous removal of zinc and cationic dye from binary hazardous mixtures, *Chem. Eng. J.* 259 (2015) 438–448.

- [40] I. Langmuir, The adsorption of gases on plane surfaces of glass, mica and platinum, *J. Am. Chem. Soc.* 57 (1918) 1362–1403.
- [41] K. Kumar, V. Ramamurthi, S. Sivanesan, Modeling the mechanism involved during the sorption of methylene blue onto fly ash *J. Colloid Interface Sci.* 284 (2005) 14–21.
- [42] B. Noroozi, G.A. Sorial, H. Bahrami, M. Arami, Equilibrium and kinetic adsorption study of a cationic dye by a natural adsorbent—Silkworm pupa, *J. Hazard. Mater.* 139 (2007) 167–174.
- [43] O. Hamdaoui, Batch study of liquid-phase adsorption of methylene blue using cedar sawdust and crushed brick, *J. Hazard. Mater.* 135 (2006) 264–273.
- [44] R. Han, D. Ding, Y. Xu, W. Zou, Y. Wang, Y. Li, L. Zou, Use of rice husk for the adsorption of congo red from aqueous solution in column mode, *Bioresour. Technol.* 99 (2008) 2938–2946.
- [45] K.R. Hall, L.C. Eagleton, A. Acrivos, T. Vermeulen, Pore- and solid-diffusion kinetics in fixed-bed adsorption under constant-pattern conditions, *Ind. Eng. Chem. Fundam.* 5 (1966) 212–223.
- [46] H. Freundlich, Über die adsorption in lösungen (Over the adsorption in solution), *Z. Phys. Chem.* 57 (1906) 384–470.
- [47] D. Ozdes, C. Duran, H.B. Senturk, H. Avan, B. Bicer, Kinetics, thermodynamics and equilibrium evaluation of adsorptive removal of methylene blue onto natural illitic clay mineral, *Desalin. Water Treat.* 52 (2014) 208–218.
- [48] R.E. Treyball, *Mass Transfer Operations*, second ed., Mc Graw Hill, New York, NY, 1968.
- [49] Y.S. Ho, G. McKay, Sorption of dye from aqueous solution by peat, *Chem. Eng. J.* 70 (1998) 115–124.
- [50] M.A. Al-Ghouti, M.A.M. Khraisheh, M.M.M. Ahmad, S. Allen, Adsorption behaviour of methylene blue onto Jordanian diatomite: A kinetic study, *J. Hazard. Mater.* 165 (2009) 589–598.
- [51] Y. Liu, Y. Kang, B. Mu, A. Wang, Attapulgit/bentonite interactions for methylene blue adsorption characteristics from aqueous solution, *Chem. Eng. J.* 237 (2014) 403–410.
- [52] M. Gouamid, M.R. Ouahrani, M.B. Bensaci, Adsorption equilibrium, kinetics and thermodynamics of methylene blue from aqueous solutions using date palm leaves, *Energy Proc.* 36 (2013) 898–907.
- [53] M. Otero, F. Rozada, L.F. Calvo, A.I. García, A. Morán, Kinetic and equilibrium modelling of the methylene blue removal from solution by adsorbent materials produced from sewage sludges, *Biochem. Eng. J.* 15 (2003) 59–68.
- [54] O. Dülger, F. Turak, K. Turhan, M. Özgür, Sumac leaves as a novel low cost adsorbent for removal of basic dye from aqueous solution, *ISRN Anal. Chem.* 2013 (2013) 9 (Article ID 210470). Available from: <<http://dx.doi.org/10.1155/2013/210470>>.
- [55] S.J. Allen, Q. Gan, R. Matthews, P.A. Johnson, Kinetic modeling of the adsorption of basic dyes by kudzu, *J. Colloid Interface Sci.* 286 (2005) 101–109.
- [56] W.T. Tsai, J.M. Yang, C.W. Lai, Y.H. Cheng, C.C. Lin, C.W. Yeh, Characterization and adsorption properties of eggshells and eggshell membrane, *Bioresour. Technol.* 97 (2006) 488–493.
- [57] S. Lagergren, About the theory of so called adsorption of soluble substances, *Kungl. Svenska Vetenskapsakad. Handlingar* 24(4) (1898) 1–39.
- [58] Y.S. Ho, G. McKay, A Comparison of chemisorption kinetic models applied to pollutant removal on various sorbents, *Process Saf. Environ. Prot.* 76(4) (1998) 332–340.
- [59] Y.S. Ho, G. Mc Kay, The kinetics of sorption of divalent metal ions onto sphagnum moss peat, *Water Res.* 34 (2000) 735–742.
- [60] Y.S. Ho, G. Mckay, Kinetic models for the sorption of dye from aqueous Solution by wood, *Process Saf. Environ. Prot.* 76(2) (1998) 183–191.
- [61] Y.S. Ho, G. McKay, Kinetic model for lead (II) sorption on to peat, *Adsorpt. Sci. Technol.* 16(4) (1998) 243–255.
- [62] W.J. Weber Jr., J.C. Morris, Kinetics of adsorption on carbon from solution, *J. Sani. Eng. Div. Ame. Soc. Civ. Eng.* 89 (1963) 31–60.
- [63] V.J.P. Poots, G. McKay, J.J. Healy, The removal of acid dye from effluent using natural adsorbents—I peat, *Water Res.* 10(12) (1976) 1061–1066.
- [64] W.H. Cheung, Y.S. Szeto, G. McKay, Intraparticle diffusion processes during acid dye adsorption onto chitosan, *Bioresour. Technol.* 98 (2007) 2897–2904.